RSC Advances

ROYAL SOCIETY OF CHEMISTRY

www.rsc.org/advances

DNA Templated Self-assembly of Gold Nanoparticles Cluster in Colorimetric Detection of Plant Viral DNA using Gold Nanoparticles Conjugated Bi-functional Oligonucleotide Probe

G. Dharanivasan,[a] S.U. Mohammed Riyaz,[a] D. Michael Immanuel Jesse,[a] T. Raja Muthuramalingam,[a] G. Rajendran[a] and K. Kathiravan [a*]

[a] Department of Biotechnology, University of Madras, Guindy Campus, Chennai 600 025, Tamil Nadu, India

Corresponding Address

e-mail: kathir68@rediffmail.com; drkkathiravan@gmail.com

Abstract

DNA templated self-assembly of gold nanoparticles clustered in different configurations (n = 2–∞) was investigated in colorimetric detection of ToLCNDV DNA using gold nanoparticle conjugated bifunctional oligo probe. AuNP- bifunctional oligonucleotide probe conjugate was prepared using citrate capped AuNPs (~19 nm) and virus specific ssoligo probes 1 and 2. Each conjugate consisting of ~ 105 ssoligo probes 1 and 2 specific for forward and reverse strands of PCR amplified ToLCNDV dsDNA target. The intensity of UV-visible absorbance spectra of AuNP-bifunctional oligonucleotide probe decreased gradually after hybridization with different ratios of dsDNA targets (0.0–1.0). Hybridized AuNP-bifunctional oligonucleotide probes showed gradual resistance against salt induced aggregation while increasing concentrations of dsDNA target upto the ratio of 1.0. The color of solution was remain in red even after hybridization of AuNP-bifunctional oligonucleotide probe with dsDNA target. These hybridized AuNP-bifunctional oligonucleotide probes were found as clusters with different configurations (n = 2–11) in a defined interparticle distance (1.3–2.1 nm). This target DNA guided self-assembly of AuNP-bifunctional oligonucleotide probes is

the reason for different optical absorbance properties of hybridized solution before and after the salt treatment. Exciting finding of this investigation is that, the number of anchored AuNP-bifunctional oligonucleotide probe on center core particle tends to form a AuNPs cluster that varied from 1–6 and extended to 8 and 10 with an increasing size of core particle diameter. Three dimensional DNA templated AuNP cluster assembly in flower and pyramid shapes was possible in dsDNA target with AuNP-bifunctional oligonucleotide probe but not in AuNP- monofunctional oligonucleotide probe. Limit of detection sensitivity of this bi-functional nanoprobe assay was ~ 7.2 ng. Also, this AuNP-bifunctional oligonucleotide probe can reduce the concentration of target DNA required for colorimetric detection to half as it can recognise both strands in dsDNA target at simultaneously. The proof of this concept will be used for further development of ultra sensitive nanoassay method and also applicable for material science applications.

Keywords

AuNP-bifunctional oligonucleotide probe, AuNP cluster assembly, Hybridization and salt induced aggregation.

Introduction

Nanotechnology emphasizes materials in 10^{-9} meter scales, involving biotechnology, material sciences and engineering applications.[1] In last decades, metal nanoparticles have been widely used in the field of biosensor,[2,3] nanoassembly,[4,5] and nanoelectronics.[6,7] Particularly, gold nanoparticles (AuNPs) are extensively used in molecular diagnosis[8–10] because of their interesting physicochemical properties.[11–13] The discovery of nanoparticles conjugated oligonucleotide/ DNA (AuNPs-DNA) made a significant development in the field of clinical diagnosis through colorimetric detection of target DNA,[8–10, 14] single base mismatch,[15–18] deletion and insertion,[19] *E.coli* genomic DNA,[20] *White spot syndrome virus*[21] detection and discrimination of *Mycobacterium tuberculosis.*[22–24] Where, AuNPs acting as an optical sensing element and oligonucleotide probe serves as a recognition unit. Recently, AuNPs conjugated oligonucleotide probes have been used for the detection of specific DNA sequence in PCR amplified DNA.[25] The hybridization of AuNPs conjugated oligonucleotide probe with its target DNA leads to self-assembly of plasmonic nanoparticles in defined three dimensional structure and/or configuration. This DNA templated self-assembly of AuNPs has been used to prepare new type of biomaterials. Also, it is a new area of research in the field of bio-nanotechnology. Because, it is a merging research field of DNA and metal colloids chemistries.[8,26] DNA mediated self assembled binary nanoparticles network materials were prepared in defined geometry using thiol modified two different oligonucleotide probes functionalized on two different sizes of AuNPs and DNA linkers.[27] Recently, triangle and square cyclic assembly of AuNPs was achieved using DNA as template.[28] Different sizes of nanomaterials in self assembled nanonetwork, posses different SPR and SERS signal characteristics which were used in the development of biosensor.[29,30] So far two different sizes of AuNPs and oligoes with mono-functionality were used to prepare DNA templated assembled nanoclusters and the detection of target DNA. Mono-functional AuNP

oligonucleotide probe is used to recognize a target sequence from any one strand of dsDNA target and another strand left as free. In order to detect another strand of dsDNA target, it requires another mono-functional AuNP-oligonucleotide probe conjugate. To address this, we hypothesized that AuNP-oligonucleotide probe conjugate with bi-functionality is used for the detection of both strands of dsDNA at the same time. Because, the selected probes hybridize both strands of dsDNA targets and tend to form a defined geometry nanoclusters. This could be reduced the concentration of target DNA and the types of nanomaterials required for the development of detection methods. Because, AuNP conjugated bi-functional oligonucleotide probe has two different oligo probes which are specific for both strands of dsDNA targets.

Moreover, the application of nanotechnology in agriculture is still at an initial stage. Specifically, nanosensor based detection of plant pathogens is not yet reported so far. Particularly, plant viruses are major causative agents for many diseases in commercial crops as well as other plants. Hence, white-fly transmitted single strand circular DNA *Tomato leaf curl virus* (ToLCV) belongs to genus of Begomovirus and family of Geminivirdeae causing severe leaf curl disease in tomato throughout the world including India and it leads 80–100 % yield loss.[31,32] Existing conventional methods like PCR and immunoassay has its own disadvantages.[2,25,33,34] Therefore, development of cost effective detection method is to be considered as very important for the early detection of viruses to control the disease. Herein, we demonstrated our hypothesis of DNA templated 3D cluster assembly of AuNP conjugated bi-functional oligonucleotide probe in the sequence specific colorimetric detection of Tomato leaf curl New Delhi virus (ToLCNDV) dsDNA targets (Figure 1).

Materials and methods

Materials: Trisodium citrate, hydrogen tetrachloroaurate trihydrate ($HAuCl_4 \bullet 4H_2O$), disodium hydrogen phosphate (Na_2HPO_4), monosodium dihydrogen phosphate (NaH_2PO_4), and sodium chloride (NaCl) were obtained from Loba Chemie (Mumbai, India). Ethylene diamine tetraacetic acid (EDTA) and agarose were purchased from HiMedia Laboratories Pvt. Ltd. (Mumbai, India). The primers encoding the coat protein (CP) gene (ToLCVFP/ ToLCVRP) synthesized commercially (Eurofins MWG Operon, India Pvt. Ltd., Bangalore, India). Red dye PCR Master Mix was purchased from Ampliqon A/S (Denmark, Germany). Polymerase Chain Reaction (PCR) was performed in L1996GGD Peltier Model Thermocycler purchased from Lark Innovative Fine Teknowledge Pvt. Ltd. (India). Thiol modified oligonucleotide probes were purchased from VBC-Biotech Service GmbH, (Vienna, Austria).

Synthesis and characterization of citrate capped AuNPs

Citrate capped AuNPs were synthesized based on the previously described boiling method.[35] In brief, 250 mL of round-bottom glass flask, a reflux condenser, and a large stir-bar washed with aqua regia (3: 1, Conc HCl: Conc HNO_3 v/v) followed by thoroughly washed with water. The glassware assembled on a heating mantle and a magnetic stirrer, and put the stir-bar in the flask. 100 mL of 1mM $HAuCl_4$ was added to flask and boiled the solution to reflux (100 °C) with vigorous stirring. Then, 5 mL of 38.8 mM sodium citrate was added to the solution at once and continue to boiling the solution for 20 min. When, yellow color of solution turns to purple and then to deep red which indicated the formation of AuNPs. Then, the solution was cooled at RT and filter through 0.45 μm nylon filter. Finally, the solution was stored at RT in a glass container in the dark place. The solution cooled at RT and characterized by UV-visible spectrophotometry (ShimadzuUV-1600, Japan).

The size and shape of the synthesized AuNPs were analyzed by HR-TEM [(model Fei Technai G^2 F30 S-TWIN) with 200 kV high-resolution (UHR) pole piece]. AuNPs solution (2 μL) was dropped on a carbon coated copper grid and dried in air at RT. Then, copper gird was placed in the sample holder and HR-TEM operated at an accelerating voltage of 200 kV with high-resolution (UHR) pole piece, lattice images were recorded. Hydrodynamic diameter and size distribution of synthesized AuNPs were analyzed using Malvern particle size analyzer (Zetasizer Nano S). AuNPs solution (2 mL) was taken in a disposable cuvette and placed in sample holder. Particle size analyzer operated at an accelerating 100 VA at 25 °C, count rate 232 kcps with duration of 60 s. The data were recorded by Zetasizer Ver. 620.

The concentration of synthesized AuNPs was calculated theoretically with the help of particles diameter and molar concentration of gold salt solution.[36] Assumed that NPs were spherical in shape and uniform in size, the average number of gold atoms per nanoparticle calculated using the following equation $N = (R_{cluster} / R_{atom})^3$. Where $R_{cluster}$ – is the diameter of NP in nanometer obtained from TEM analysis and R_{atom} = 0.137 nm – is the diameter of gold. From the result of N, the amount of nanoparticles formed (N_{NP}) in a given concentration of gold salt solution (1 dm^3 or 1 L of 1 mM: Moles of $HAuCl_4$ = 1 x 1 x 10^{-3} = 1 x 10^{-3} mol) reduced by citrate was calculated through the estimation of number of gold atoms presented in a given solution using equation N_{atom} = Moles of $HAuCl_4$ x N_A, where N_A – (Avogadro number - 6.022 x 10^{23}). From the findings of N and $N_{atom,}$ the total number of NPs formed in given solution was calculated through equation $N_{NP} = N_{atom} / N$. Hence, the final concentration of the gold colloid (C_{NP}) was estimated by dividing N_{NP} through Avagadro's number (N_A): $C_{NP} = N_{NP} / N_A$ in mol dm^{-3} (1 L).

Preparation of AuNP conjugated bi-functional oligonucleotide probe

The synthesized AuNPs solution was used for the preparation of AuNP conjugated bi-functional oligonucleotide probe. ToLCNDV specific probes sequences were designed through the multiple sequence alignment of retrieved nucleotide sequences of different isolates of ToLCNDV from NCBI. The identical and its complementary sequences were selected from two different regions for the synthesis of probes and positive control from the results of multiple sequence alignment using BioEdit software. The selected sequences were subjected to self complementation and dimer formation analyses through online tools. The designed probes (Forward probe 1 – 26 mer HS-5' -GAATTCATGTCSAAGCGWCCRGCAGA-3' and Reverse probe 2 – 26 mer HS-5'-GGTACCATTCTTMACAGTWGCAGTGC-3') were custom synthesized with thiol functional group at 5' end for the preparation of conjugates.

AuNP conjugated bi-functional oligonucleotide probe was prepared based on the earlier described method with slight modifications.[37,38] In detail, 50 pM of probe 1 for forward strand and 50 pM of probe 2 for reverse strand were mixed with 0.1 M of Phosphate-buffered saline (PBS) (10 mM of NaCl with 0.01% SDS, pH 7) and volume was made up to 1 mL with of citrate capped AuNPs and incubated at 50 °C for 24 h. After the incubation, the solution was subjected to aging process using 1 M of NaCl as the final concentration with phosphate buffer (pH 7) for 24 h at 50 ºC. Unbounded probes were removed from the solution by centrifugation at 14,000 rpm for 25 min and the supernatant was replaced with 1 mL of the phosphate buffer for two times. The centrifugate was collected and redispersed into 0.5 mL using phosphate buffer to make a stock solution, which was used for further experiments. The amount of DNA probes immobilized on the AuNPs surface was calculated

by measuring optical absorbance at 260 nm using UV-visible spectrophotometer. Morevoer, the prepared AuNP bifunctional probe was also characterized by HR-TEM and DLS.

AuNP conjugated bi-functional oligonucleotide probe was characterized by Raman spectroscopy (Raman-11; Nanophoton, Japan) after a coating with Raman probe (Rodamine 6G- R6G).[39] The conjugated solution was concentrated by centrifugation at 10,000 rpm for 15 min. Supernatant was discarded and oily red color pellet was diluted with 500 μL of 20 μM R6G and incubated for 4 h at RT. Unbounded R6G was removed by centrifugation at high speed for 15 min, the pellet was collected and diluted with 100 μL ddH_2O. The solutions were spotted on a cleaned glass slide and dried in air at RT. The samples were subjected to confocal Raman microscopy analysis by the illumination of laser light (532 nm) at 40 mW for the excitation as well as imaging. Finally, scattered lights spectra were recorded and images were captured using CCD camera.

Isolation and amplification of ToLCNDV DNA

Total genomic DNA was extracted from ToLCNDV infected tomato leaf sample based on previously described method.[40] The isolated DNA was analyzed by 0.8% agarose gel electrophoresis and quantified by UV-visible spectrophotometer. 800 bp of the CP gene fragment was amplified from ToLCNDV DNA with geminivirus specific common primers using PCR. The reaction mixture was prepared to the total reaction volume of 50 μL by the addition 25 μL of 2x red dye PCR Master Mix, 22.5 μL DNase/RNase free deionized water, ToLCV specific primers (100 pM of 0.625 μL forward primer and 0.625 μL reverse primer) and 1.25 μL of template DNA. The amplification program consist the following steps which are the initial denaturation at 94 ºC for 5 min followed by denaturation at 94 ºC for 1 min, annealing at 60 ºC for CP gene (ToLCVFP/ToLCVRP) for 1 min, extension at 72 ºC for 2 min with 25 cycles and a final extension at 72 ºC for 5 min. Amplified PCR products were

extracted from the reaction mixture by addition of 5 μL of sodium acetate solution (pH 4.2) and 100 μL of 95 % ethanol to 50 μL of the PCR reaction tube. The mixture was vortexed gently and incubated at −20 ºC for 40 min. Then the mixture was centrifuged at 10,000 rpm for 20 min. The supernatant was discarded carefully and the pellet washed with 70 % (v/v) ethanol. After washing, the pellet was air dried at RT and suspended in 50 μL RNase/DNase free deionized water for further studies. Extracted products were electrophoresed in 1.2 % (w/v) agarose gel, visualized under the UV light and quantified using UV-visible spectrophotometer. This extracted DNA was used for further experiments.

Hybridization assay and gold nanocluster self-assembly

To optimize the hybridization assay, 10 μL of AuNPs- bifunctional oligonucleotide probe was mixed with different concentrations of NaCl (0–6 M) in the presence of 5 μL of hybridization buffer (10 mM phosphate buffer, 0.1 M NaCl containing 1 mM EDTA; pH 7.2), and the volume was made up to 20 μL using deionized water. The solution was mixed well and kept for 10 min at RT. Subsequently, the absorbance was measured using UV-visible spectrophotometer and the salt concentration was optimized for the hybridization assay. Different concentrations of PCR amplified dsDNA target (0.0, 0.2, 0.4, 0.6, 0.8 and 1.0 ratios v/v) were mixed with AuNP conjugated bifunctional oligonucleotide probe and incubated initially at 95 ºC for 5 min followed by another round of incubation at 37 ºC for 55 min in the presence of hybridization buffer. After the incubation, optimized concentration of salt was added to the solution and kept at RT for 10 min and the color changes were observed. Optical absorbance of all the solutions were analyzed by UV-visible spectrophotometer before and after the addition of salt. After the hybridization assay, completely hybridized (1.0 ratio) and control samples were also analyzed by HR-TEM.

Results and discussion

Synthesis and characterization of citrate capped AuNPs

AuNPs were synthesized according to previously described method.[35] In brief, the yellow color of the reaction solution ($HAuCl_4$) was gradually changed to purple and then to red after the addition of sodium citrate at the boiling condition which indicates that the formation of AuNPs as shown in Figure 2A. Where, sodium citrate acts as reducing as well as capping agent which is controlled the further nucleation growth of NPs.[41,42] The intense red color of synthesized AuNPs is due to the interaction of incident light with a collective oscillation of free electrons in the particles (localized surface plasmon resonance-SPR).[43] The synthesized AuNPs solution was analyzed by UV-visible spectrophotometer. The maximum absorbance for red colored AuNPs solution was found at 520 nm with the sharp peak as shown in Figure 2B. This is mainly due to the size dependent SPR of metal nanoparticles.[44,45]

The size and shape of synthesized AuNPs were analyzed by HR-TEM. Figure 2C HR-TEM image shows monodispersed spherical AuNPs with diameter of ~19 nm. The growth of spherical nanoparticles take place by the reduction and subsequent deposition of reduced Au^0 metal atoms. Intially, reduced metal forms a cluster followed by continuous deposition for the growth of particles in a defined shape and size, which is regulated by capping agent.[41,46,47] Hydrodynamic diameter of synthesized citrate capped AuNPs was also revealed using DLS method. The average hydrodynamic diameter of synthesized AuNPs was found to be ~30 nm as shown in Figure 2D. Measurement of particle size by DLS method was found to be higher than particles size measured by HR-TEM method. This is due to the presence of layer of hydrogen bonds between particles surface and solvent.[48] Molar concentration of synthesized citrate capped AuNPs was calculated based on previously described method.[36] Initially, the average number of gold atoms per nanoparticle was calculated using the diameter of

synthesized AuNPs (D= ~19 nm). The number of gold atoms per nanoparticle "N" was found to be 2667418.5. From the result of N, the total number of nanoparticles (N_{NP}) formed in a given molarity of solution (1 x 10^{-3} mol) of $HAuCl_4$ was calculated (N_{NP} = 2.26 x 10^{13}). The final concentration of AuNPs (C_{NP}) was estimated by N_{NP}/Avagadro's number (N_A) and concentration of AuNPs was found to be C_{NP} = ~ 3.75 x 10^{-9} mol dm^{-3} (1 L) or 3.75 nmol. AuNPs concentration is vary accordingly to the size of particles in diameter. As increases in the number of gold atoms per nanoparticle is leads to decrease in the concentration of AuNPs.

Preparation of AuNP conjugated bi-functional oligonucleotide probe

AuNP conjugated bi-functional oligonucleotide probe was prepared based on Au-SH chemistry.[37,38] 5' thiol modified oligonucleotide probe was chemisorbed and formed thiol monolayer on the AuNPs surface as depicted in Figure 1. Chemisorption of thiol modified oligo probes 1 and 2 on AuNPs surface was enhanced by reducing the intermolecular and interparticle repulsion forces between ssDNA oligonucleotide probes and AuNPs using PBS.

Oligo thiol attached AuNPs shows strong resistance against salt induced aggregation in aging process and unbounded AuNPs get aggregated. Figure 3A, photographic image shows synthesized AuNPs as reference (a), AuNP conjugated bi-funcional oligonucleotide probe (b) and (c) aggregated AuNPs as control. Intense red color of AuNPs in aqueous solution is due to the negative repulsion force based monodispesity and SPR.[49] After the addition of salt, a complete aggregation of AuNPs was found only in solution 'c' and color of the solution was changed to blue. Whereas, this color change was not observed in solution 'b' (AuNP conjugates bi-functional oligo probe) even in the presence of high salt concentration. Particles in solution 'b' were found to be monodisperse and red in color. It proves that ssoligo probes 1 and 2 were attached on AuNP surface through Au-SH chemistry and tend to form a thiol monolayer on NPs. Because, thiol groups show the high affinity towards noble metal

surfaces, particularly gold.[50,51] In addition, surface bound ssDNA oligo probes enhance interparticle electronegative repulsion force between NPs and it helps to maintain an appropriate interparticles distance between the conjugates and it prevents the aggregation.[52,53] Optical absorbance properties of AuNP conjugated bi-functional oligonucleotide probe was analyzed by UV-visible spectrophotometer with control and reference. Figure 3B shows UV-visible absorbance spectra 'a', 'b' and 'c' for AuNPs (Ref), AuNP conjugated bi-functional oligonucleotide probe (b) and AuNPs (control) (c) after the aging process, respectively. AuNPs shows different light absorbance properties with and without the salt treatment. In the absence of salt, AuNPs show sharp peak at 520 nm with higher intensity (Fig. 3B spectra 'a'). In the presence of salt, AuNPs show broadening peak towards longer wavelength region (above 600 nm) with small peak at 520 nm (Fig. 3B specta 'c'). This peak broadening could be due to the aggregation, color changes and SPR band shift of AuNPs.[54] Absorbance spectra of AuNP conjugated bi-functional oligonuclotide probe shows SPR band at 524 nm even after the salt treatment (Fig. 3B spectra 'b'). The red shift of AuNPs was found from 520 nm to 524 nm after the conjugation of AuNPs with thiol modified oligonucleotide probes. This could be due to the change of refractive index surrounding of AuNPs and the formation of dielectric layers around AuNPs.[55] Further, it implies that successful chemisorption of ssDNA probes onto the surface of AuNPs.[53,56,57] It also increases the electronegativity and stability of AuNPs- conjugated probe, significantly.[58]

Confocal Raman microscopy have been used to analyze the surface of AuNPs bi-functional oligonucleotide probe using Rhodamine 6G (R6G) as Raman probe. SERS spectra of R6G, R6G with AuNPs and AuNP conjugated bi-functional oligonucleotide probe as shown in Figure 3C. Raman probe R6G showed major peaks at 608, 769, 1186, 1357, 1533, 1565 and 1645 cm^{-1} which are the characteristic peaks of C–C–C, C–H, C–C, C–N and ring plane assignments of R6G.[39] Raman probe bounded AuNPs shows slight shift of SERS peaks

(± 2–6 cm^{-1}) at 608 → 610 cm^{-1}, 918→920 cm^{-1}, 1017→ 1013 cm^{-1}, 1121→ 1119 cm^{-1}, 1186 → 1188 cm^{-1}, 1299 → 1305 cm^{-1}, 1357 → 1359 cm^{-1}, 1413 → 1417 cm^{-1}, 1500 → 1502 cm^{-1},1533 → 1531 cm^{-1},1593 → 1591 cm^{-1} with enhanced intensity and new peak was appeared at 824 cm^{-1} (Fig. 2C, AuNPs + R6G spectra). This could be due to the adsorption of $R6G^{+}$ molecules on AuNPs surface through electrostatic forces. Enhancement of SERS bands from 500 – 2000 cm^{-1} by the result of parallel to inclined orientational change which can enhance Raman bands from vibrational modes that perpendicular to the xanthines plane mode. It suggests that R6G molecules show closed proximity with Au metal surfaces. Because, it may locate 0–4 nm close to the substrate surface or the electromagnetic field. These interactions between R6G and AuNPs surfaces cause larger scattering which may lead to changes in the Raman spectra.[59–61] Similarly, thiol modified oligonucleotide probe functionalized AuNP with R6G spectra showed SERS band shifts like 1184, 1355, 1529, 1568 and 1643 cm^{-1} (Fig. 3C, AuNP-bifunctional oligonucleotide probe conjugate with R6G). The intensity peaks of R6G bound AuNP conjugated bi-functional oligonucleotide probe is lower than the AuNPs with R6G peak intensity and higher than the R6G peaks intensity except at 551 and 918 cm^{-1}. However, the intensity of SERS peaks was gradually increased in the order from R6G to AuNP- bifunctional oligonucleotide probe conjugate+R6G and to AuNPs + R6G. The number of R6G molecules bound on the surface of AuNPs could be the reason for increase in the intensity of SERS peaks in the abovesaid order. SERS peaks intensity at 1500 and 1645 cm^{-1} is proportional to the number of Raman probe bound on the AuNPs surface. Number of R6G molecules bound on the unmodified AuNPs surface was found to be very high. This could be a reason for increase in the peaks intensity of AuNPs + R6G when compared with R6G spectra. SERS peaks shift was occurred due to the weaker interactions of R6G on AuNPs surface in inclined plane. Decreased intensity of SERS peaks of AuNP conjugated bi-functional oligonucleotide probe with R6G

is might be due to the presence of thiol monolayer and nonspecific interactions of oligonucleotide probes on AuNPs surface in flat plane orientation. This might be interfered with the interaction of R6G molecules with AuNPs surface. The shifts of SERS peaks with decreased intensity of AuNP conjugated bi-functional oligonucleotide probe is due to the result of chemisorptions of ssoligo probes.[62,63] The corresponding Raman confocal images of R6G and R6G with AuNPs, AuNP conjugated bi-functional oligonucleotide probe as shown in Figure 3C inset image with scale bar. Intense red, pink and blue color indicates that the presence of R6G, AuNPs and clean surface, respectively.

AuNP conjugated bi-functional oligonucleotide probe was also investigated by HR-TEM. Figure 3D represents HR-TEM images of AuNP conjugated bi-functional oligonucleotide probe in two dimensional arrangements. This 2D arrangements of AuNP-bifunctional oligonucleotide probe conjugates were mainly due to the weaker interactions between the conjugates. Figure 3C inset image shows the presence of a thin outer layer of 1.6 nm around the nanoparticle. It also proves that the presence of surface bound oligonucleotide probes which favour of 2D assembly of NPs.[8,64] Dispersibility and aggregation of AuNP conjugated bi-functional oligonucleotide probe in high salt concentration were analyzed by measuring hydrodynamic diameter of particles in aqueous medium through DLS along with control and reference as shown in Figure 3E. The average hydrodynamic diameter of AuNP conjugated bi-functional oligonucleotide probe after the salt treatment was found to be ~65 nm. This clearly shows that AuNP conjugated bi-functional oligonucleotide probe resist the salt induced aggregation. This could be due to the functionalization of probe which increases the electronegativity and stability of AuNPs in high salt concentration. However, the sizes of AuNP conjugated bi-functional oligonucleotide probe was two fold higher than the size of

synthesized AuNPs. This could be due to the weaker interactions between AuNP-bifunctional oligonucleotide probe conjugates.

Quantification of surface bound oligonucleotide probes on AuNPs

Number of oligonucleotide probes chemisorbed on a AuNP surface (~19 nm) was calculated with aid of UV-visible spectroscopy method. AuNP conjugated oligonucleotide probes were treated with β-mercaptoethanol and salt. Where, β-mercaptoethanol is a strong reducing agent breaks Au−SH bond between NPs and ssoligos. Then, AuNPs was aggregated and ssoligos were released to the solution. Optical absorbance of collected supernatant at 260 nm was measured and it was found to be 1.62 OD. Total weight of ssoligo bound on AuNPs surface was calculated to 32.4 μg (ssOligo: 1 at OD_{260}, Unit = 20 μg). Using this, molar concentration of immobilized oligomers was calculated and it was found to be 3.96 x 10^{-9} M, Number of ssoligo probes present in the given concentration of ssoligo stock solution was calculated (23.8 x 10^{14}). With assistance of molar concentration of AuNPs and number of AuNPs present in the solution, the number of oligonucleotide probes immobilized on a AuNP was calculated and it was found to be ~105 numbers. The number of ssoligo probes immobilized on AuNP is depends on the length of oligomer, size and surface area of particles. The number of ssoligo probes bound on NP surface was increased while increasing the size of nanoparticles. Similarly, short oligomer can be conjugated in faster with higher numbers than the longer length. This is due to the inter-strand steric interference between ssoligos and self coiled secondary structure of long ssoligos.[65–67]

Hybridization assay and DNA guided gold nanoparticles cluster self-assembly

The salt concentration was optimized for the complete aggregation of AuNP conjugated bi-functional oligonucleotide probe using different concentrations of NaCl (0−6

M). Figure 4A photographic image shows the color of AuNP conjugated bi-functional oligonucleotide probe changed from red to purple and blue after the addition of NaCl. The color of AuNP conjugated bi-functional oligonucleotide probe was found in purple at 2 and 3 M NaCl which was completely changed to blue at 4 M NaCl and above. The complete aggregation and black precipitation of AuNPs was found at 6 M. From these results, 4 M NaCl was taken as optimizied salt concentration for further hybridization assay which is approximately four times higher than the NaCl required for the complete aggregation of unfunctionalized AuNPs. The corresponding UV-visible absorbance spectra of different concentrations of salt (0−6 M) treated AuNP conjugated bi-functional oligonucleotide probe as shown in Figure 4B. Absorbance maxima of AuNP-bifunctional oligonucleotide probe was found at 525 nm which has gradually decreased with SPR band shift towards longer wavelength (above 600 nm) while increasing the concentration of NaCl from 1 M to 6 M. A significant SPR shift was started from 4 M to 6 M NaCl and it indicated the complete aggregation of AuNP- bifunctional oligonucleotide probe conjugate. This color transition of AuNP- bifunctional oligonucleotide probe conjugates was mainly due to the salt induced aggregation.[68]

Double stranded target DNA was amplified from ToLCNDV infected positive sample using ToLNDV CP gene specific primers (ToLCVFP/ToLCVRP) and analyzed by 1.2% agarose gel electrophoresis. Amplified PCR product was extracted, quantified spectrometrically (180.4 ng/μL) and 100 times diluted PCR DNA used for further study (data not shown). AuNP-bifunctional oligonucleotide probe conjugate was subjected to hybridization with PCR amplified dsDNA target of ToLCNDV CP gene in different ratios (0.2, 0.4, 0.6, 0.8 and 1.0 v/v). Figure 5A shows hybridized AuNP-bifunctional oligonucleotide probe with dsDNA target in different ratios without any significant color

changes and all were observed in red color. But, the corresponding UV- visible spectra shows that gradual decreases in the intensity of absorbance at 525 nm while increasing concentration of dsDNA targets from ratio 0.2 to 1.0 (Fig. 5B spectra 'a-e'). This is due to the distance dependent surface plasmon resonance of hybridized AuNP- bifunctional oligonucleotide probe with its dsDNA target.

AuNP-bifunctional oligonucleotide probe with 0.2 ratio of target dsDNA and control showed the absorbance maximum at 525 nm with high intensity which indicates the interpartilce distance between AuNP- bifunctional oligonucleotide probe conjugates could be found in maximum. Because, the number of unhybridized AuNP- bifunctional oligonucleotide probe is greater than the number of hybridized AuNP- bifunctional oligonucleotide probe conjugate with dsDNA target at lower concentration. The unhybridized AuNP- bifunctional oligonucleotide probes in solution repulse to each other and it maintains maximum interparticles distance. This could be influenced by the maximum absorbance of incident light rather than the scattering. While increasing the concentration of dsDNA target up to ratio 1.0, AuNP- bifunctional oligonucleotide probe conjugates were completely hybridized with its target to form a satellite like gold nanoparticle cluster structure which leads to significant reduction of interparticles distance.[65,69] This could increase the scattering of incident light rather than the absorbance as a result the intensity of absorbance was gradually reduced significantly from ratio 0.2 to 1.0 (Fig. 5C). A significant color change was observed after the addition of optimized salt concentration to the hybridized AuNP conjugated bi-functional oligo probe – dsDNA targets complex solutions. The color of AuNP- bifunctional oligonucleotide probe conjugate solution in red was completely changed into blue at ratio 0.0 after the addition of 4 M NaCl as shown Figure 6A. This is due to salt induced aggregation of AuNP-bifunctional oligonucleotide probe by the complete absence of target DNA. The degree of salt induced aggregation was reduced significantly and bluish

light purple color of AuNP- bifunctional oligonucleotide probe solution at ratio 0.2 was gradually retains its original redish purple color while increasing the concentration of target DNA from ratio 0.2, 0.4, 0.6, 0.8 and 1.0 as shown Figure 6A. After the hybridization of AuNP- bifunctional oligonucleotide probe and with targets, small stretches of double helix structure was formed between the probe and target which provides a strong resistance force against salt induced aggregation and maintains significant interparticles distance between AuNP- bifunctional oligonucleotide probes. This also prevents particles aggregation and overlapping. An optical absorbance properties of corresponding hybridized solutions (Ref, ratios at 0.0, 0.2, 0.4, 0.6, 0.8 and 1.0) were shown in Figure 6B UV-vis spectra 'a-f', respectively. The intensity of optical absorbance at 525 nm for spectra 'a-f' were found to be increased gradually as the concentrations of dsDNA target increased from 0.0 to 1.0 ratios, respectively after the salt treatment. The absorbance intensity of 'Ref' solution was found to be very high because it is free from salt treatment. Figure 6C, represents relationship between concentration of dsDNA target and optical absorbance properties of AuNP-bifunctional oligonucleotide probe. The absorbance intensity of AuNPs solutions at 525 nm was increased with respect to increase of dsDNA targets (0.0 – 1.0 ratios) at high salt concentration. This is due to increase in the number of hybridized AuNP- bifunctional oligonucleotide probe conjugates with its target dsDNA and it tend to form a satellite structure as depicted in schematic representation (Figure 1). These distance dependent SPR is reasonable for different optical absorbance properties of hybridized AuNP- bifunctional oligonucleotide probe conjugates with target DNA at different concentrations.[10,68] The detection sensitivity limit of this bi-functional nanoprobe assay was determined and it was found to be ~7.2 –18 ng, which is two times higher than the earlier report.[20]

While nanoparticle cluster assembly of AuNP-bifunctional oligonucleotide probe was found in the presence of targets DNA, conjugates were found to be aggregated in the absence of target DNA as shown in Figure 7A and B (HR-TEM images) respectively. Cluster like assembly of AuNP- bifunctional oligonucleotide probe was obtained by the sequence specific hybridization with its dsDNA target. Hence, AuNP-bifunctional oligonucleotide probe has probe 1 and 2 which were specific for 3' end of forward and 5' end of reverse stands of dsDNA target. Probe 1 of one conjugate get hybridized with 3' end of dsDNA target and probe 2 of another particles get hybridized with 5' end of dsDNA target. Similarly each AuNP conjugated bi-functional oligonucleotide probe has more numbers of probes 1 and 2, which were hybridized with its dsDNA target to form a very large size AuNPs cluster through DNA template self-assembly in configuration (n= ∞). The inter-particle distance (~1.3 nm to 2.3 nm) between AuNP- bifunctional oligonucleotide probe was maintained by double helix form of dsDNA target and conjugated probe at high salt concentration. Moreover, different configurations of AuNP- bifunctional oligonucleotide probe cluster assemblies were found in HR-TEM analysis after the hybridization with dsDNA target and individual cluster comprising 2−11 nanoparticles as shown in Figure 8. Nanoparticle cluster assembly of AuNP-bifunctional oligonucleotide probe consisting single AuNPs-bifunctional conjugate core anchored with mono (a), dimer (b), trimmers (c & d), tetramer (e), hexamer (f), octamer (g) and decamer (h) AuNP-bifunctional oligonucleotide probe conjugates through hybridization with dsDNA targets as shown in Figure 8 (a-h with n=2−11 configurations, respectively). In addition, a pyramid like assembly of AuNP-bifunctional oligonucleotide probe conjugate (n= 10) was observed in HR-TEM analysis (Fig. 8- i). Step-wise assembly of nanocluster was achieved by anchored six AuNP-bifunctional oligonucleotide probe conjugates with single core AuNP-bifunctional oligonucleotide conjugate in a defined nano flower like structure in the presence of dsDNA targets (Fig. 8. a-

f). However, number of AuNP- bifunctional oligonucleotide probe conjugate anchored with single core was extended to 8 and 10 due to increases in the size of core from ~19 nm to 55 nm and 63 nm, respectively. These increased size of AuNP- bifunctional oligonucleotide probe core were found accidently in TEM analysis in the form of self assembled gold nanocluster. This accidental findings proves that the increase in the size of AuNP core also increases the number of AuNPs anchoring on its surface. The defined flower-like nano gold cluster assembly was observed only in the presence of target dsDNA. It confirms that this dsDNA target guiding to nano cluster assembly of AuNP-bifunctional oligonucleotide probe through hybridization when it showed perfect complementary matche between AuNP-bifunctional oligonucleotide probe and targets.[27,70] Further, dsDNA target also guiding to pyramid like structure assembly of AuNP-bifunctional oligonucleotide probe was found in HR-TEM analysis (Fig. 8-i). Moreover interparticles distance between core and anchored AuNP-bifunctional oligonucleotide probe conjugates was found to be 0.9 nm to 1.2 nm in all assembled nanocluster structures and this could be maintained by the presence of dsDNA targets between AuNP-bifunctional oligonucleotide probe conjugates after the hybridization.

Conclusion

DNA templated 3D self-assembly of AuNPs cluster in different configurations in colorimetric detection of plant viral DNA using AuNP-bifunctional oligonucleotide probe is investigated and discussed in present work. Citrate capped gold nanoparticles of ~19 nm was synthesized for the preparation of AuNP-bifunctional oligonucleotide probe conjugates. Equal concentrations of thiolated oligo probe 1 and 2 specific for ToLCNDV CP gene were immobilized on AuNP through Au-SH chemistry. Total number of ssoligo probes 1 and 2 chemisorbed on each nanoparticle was found to be ~105 numbers. AuNP conjugated bi-functional oligonucleotide prob was used to detect both strands of dsDNA target

simultaneously. AuNP-bifunctional oligonucleotide probes hybridized with the different concentrations of ToLCNDV DNA (ratios 0.0−1.0). The intensity of optical absorbance of conjugates was gradually decreased with increase of dsDNA concentration in ratios 0.0−1.0 after the hybridization. AuNP- bifunctional oligonucleotide probe was self assembled with dsDNA target in close proximity and reduce the inter-particle distance. This leads to changes in optical absorbance properties without significant color change. After the salt treatment, free AuNP-bifunctional oligonucleotide probe aggregates and causing color changes from red to blue. Hybridized AuNP-bifunctional oligonucleotide probe was not aggregated and showed stability in high salt concentration. The resistance against salt induced aggregation was increased gradually with increasing the concentration of dsDNA target from ratio 0.2 to 1.0 and the red color was retained as such. Also this dsDNA target guiding to 3D self-assembly of gold nanoparticle cluster with different configuration (n= 2−11 and ∞) in flower and pyramid shape. The number of anchored AuNP-bifunctional oligonucleotide probe on centre core cluster is varied from 6 to 8 and 10 and it is due to increases in the size of core AuNP. The results prove that AuNP-bifunctional oligonucleotide probe detect the both forward and reverse strands of dsDNA target and reduces the concentration of DNA target required for the nanoassay. Limit of detection sensitivity of the bi-functional nanoprobe assay was 7.2 ng, which was twofold higher than earlier report. This method is simple and rapid than the existing conventional methods. This work also provide new insight for the preparation of gold nanoparticle cluster in defined shape and size using single type of AuNPs. This probe of concept helps to develop an ultra sensitive nanoassay method and preparation of gold nanoparticles cluster for material science applications.

Acknowledgments

The authors thanks to UGC [F. No. 37-440/2009 (SR)] and CSIR [F. No. 9/115(0763)/2013-EMR-I, Government of India for their financial assistance. The authors also thanks to The Director, NCNS & NT, University of Madras (UNOM) for HR-TEM and Raman 11 characterizations.

REFERENCES

1. W. Cai, T. Gao, H. Hong and J. Sun, Application of Au nanoparticles in cancer nanotechnology, *Nanotech. Sci. Appl.,* 2008, 1, 17-32.
2. N. L. Rosi and C. A. Mirkin, Nanostructures in biodiagnostics, *Chem. Rev.,* 2005, 105, 1547–1562.
3. N. C. Tansil and Z. Gao, Nanoparticles in biomolecular detection, *Nanotoday,* 2006, 1, 1-37.
4. A. Fu, C. M. Micheel, J. Cha, H. Chang, H. Yang and A. P. Alivisatos, Discrete nanostructures of quantum dots/Au with DNA, *J. Am. Chem. Soc.,* 2004, 126, 10832–10833.
5. E. D. Goluch, J. M. Nam, D. G. Georganopoulou, T. N. Chiesl, K. A. Shaikh, K. Ryu, A. E. Barron, C. A. Mirkin and C. Liu, A bio-barcode assay for on-chip attomolar-sensitivity protein detection, *Lab Chip,* 2006, 6, 1293–1299.
6. S. J. Park, A. A. Lazarides, C. A. Mirkin, P. W. Brazis, C. R. Kannewurf and R. L. Letsinger, The electrical properties of gold nanoparticle assemblies linked by DNA, *Angew. Chem., Int. Ed.,* 2000, 39, 3845–3848.
7. J. M. Nam, C. S. Thaxton and C. A. Mirkin, Nanoparticle-based bio-bar codes for the ultrasensitive detection of proteins, *Science,* 2003, 301, 1884–1886.

8. C. A. Mirkin, R. L. Letsinger, R. C. Mucic and J. J. Storhoff, A DNA-based method for rationally assembling nanoparticles into macroscopic materials, *Nature,* 1996, 382, 607–609.
9. G. P. Mitchell, C. A. Mirkin and R. L. Letsinger, Programmed assembly of DNA functionalized quantum dots, *J. Am. Chem. Soc.,* 1999, 121, 8122–8123.
10. J. M. Nam, S. I. Stoeva and C. A. Mirkin, Bio-bar-code based DNA detection with PCR-like sensitivity, *J. Am. Chem. Soc.,* 2004, 126, 5932–5933.
11. R. Shukla, V. Bansal, M. Chaudhary, A. Basu, R. R. Bhonde and M. Sastry, Biocompatibility of gold nanoparticles and their endocytotic fate inside the cellular compartment: a microscopic overview, *Langmuir,* 2005, 21, 10644–10654.
12. L. M. Liz-Marzan, Tailoring surface plasmons through the morphology and assembly of metal nanoparticles, *Langmuir,* 2006, 22, 32–41.
13. N. L. Rosi, D. A. Giljohann, C. S. Thaxton, A. K. R. Lytton-Jean, M. S. Han and C. A. Mirkin, Oligonucleotide-modified gold nanoparticles for intracellular gene regulation, *Science,* 2006, 312, 1027–1030.
14. A. P. Alivisatos, K. P. Johnsson, X. Peng, T. E. Wilson, C. J. Loweth, M. P. Bruchez jr. and P. G. Schultz, Organization of "nanocrystal molecules" using DNA, *Nature,* 1996, 382, 609-611.
15. K. Sato, K. Hosokawa and M. Maeda, Rapid aggregation of gold nanoparticles induced by non-cross-linking DNA hybridization, *J. Am. Chem. Soc.,* 2003, 125, 8102-8103.
16. K. Sato, K. Hosokawa and M. Maeda, Non-cross-linking gold nanoparticle aggregation as a detection method for single-base substitutions, *Nucleic Acids Res.,* 2005, 33, e4 1-5.

17. G. Doria, R. Franco and P. Baptista, Nanodiagnostics: fast colorimetric method for single nucleotide polymorphism/mutation detection, *IET Nanobiotechnol*., 2007, 1, 53- 57.

18. J. W. Qin and L. Y. L. Yung, Nanoparticle-based detection and quantification of DNA with single nucleotide polymorphism (SNP) discrimination selectivity, *Nucleic Acids Res*., 2007, 35, e111 1-8.

19. J. J. Storhoff, R. Elghanian, C. R. Mucic, C. A. Mirkin and L. R. Letsinger, One-pot colorimetric differentiation of polynucleotides with single base imperfections using gold nanoparticle probes, *J. Am. Chem. Soc*., 1998, 120, 1959 – 1964.

20. B. Padmavathy, R. Vinoth Kumar and B. M. Jaffar Ali, A direct detection of Escherichia coli genomic DNA using gold nanoprobes, *J. Nanobiotechnology,* 2012, 10, 8.

21. Y. Seetang-Nun, W. Jaroenrama, S. Sriurairatana, R. W. Suebsing and Kiatpathomchai, Visual detection of white spot syndrome virus using DNA-functionalized gold nanoparticles as probes combined with loop-mediated isothermal amplification, *Mol. Cell. Probes,* 2013, 27, 71-79.

22. P. Upadhyay, M. Hanif and S. Bhaskar, Visual detection of IS*6110* of *Mycobacterium tuberculosis* in sputum samples using a test based on colloidal gold and latex beads, *Clin. Microbiol. Infect.,* 2006, 12, 1118 – 1122.

23. P. Costa, A. Amaro, V. Botelho, J. Inacio and P. V. Baptista, Gold nanoprobe assay for the identification of mycobacteria of the *Mycobacterium Tuberculosis c*omplex, *Clin. Microbiol. Infect.,* 2010, 16, 1464 – 1469.

24. Y. Wen, K. C. McLaughlin, K. P. Lo, H. Yang and F. H. Sleiman, Stable Gold nanoparticle conjugation to internal DNA positions: facile generation of discrete gold nanoparticle-DNA assemblies, *Bioconjugate Chem*., 2010, 21, 1413-1416.

25. L. M. Demers, C. A. Mirkin, R. C. Mucic, R. A. Reynolds, R. L. Letsinger, R. Elghanian, H. Deng, Y. Xu, Y. Liu, Z. Che, H. Guo, S. Shan, Y. Sun, X. Liu, K. Huang, X. Ma, Y. Wu, X. J. Liang, Gold nanoparticles with asymmetric polymerase chain reaction for colorimetric detection of DNA sequence, *Anal. Chem.,* 2012, 84, 1253-1258.

26. H. Zhang, E. W. Edwards, D. Wang and H. Mohwald, Directing the self-assembly of nanocrystals beyond colloidal crystallization, *Phys. Chem. Chem. Phys.,* 2006, 8, 3288–3299.

27. R. C. Mucic, J. J. Storhoff, C. A. Mirkin and R. L. Letsinger, DNA-directed synthesis of binary nanoparticle network materials, *J. Am. Chem. Soc.,* 1998, 120, 12674-12675.

28. T. Ohshiro, T. Zako, R. W. Tamaki, T. Tanaka and M. Maeda, A facile method towards cyclic assembly of gold nanoparticles using DNA template alone, *Chem. Commun.,* 2010, 46, 6132–6134.

29. W. Yan, L. Xu, C. Xu, W. Ma, H. Kuang, L. Wang and N. A. Kotov, Self-assembly of chiral nanoparticle pyramids with strong R/S optical activity, *J. Am. Chem. Soc.,* 2012, 134, 15114−15121.

30. C. T. Nguyen, T. H. Tran, X. Lu and R. M. Kasi, Self-assembled nanoparticles from thiol functionalized liquid crystalline brush block copolymers for dual encapsulation of doxorubicin and gold nanoparticles, *Polym. Chem.,* 2014, 5, 2774-2783.

31. M. K. Nakhla and D. P. Maxwell, Epidemiology and management of tomato yellow leaf curl disease. In: Hadidi A., Khetarpal RK., Koganezawa H. (eds.). Plant Virus Disease Control, *The American Phytopathological Society,* St. Paul, MN, USA, 1999, pp. 565-583.

32. R. V. Chowda Reddy, J. Colvin, V. Muniyappa and S. Seal, Diversity and distribution of begomoviruses infecting tomato in India, *Arch. Virol.,* 2005, 150, 845–867.

33. S. Rho, S. J. Kim, S. C. Lee, J. H. Chang, H. –G. Kang and J. Choi, Colorimetric detection of ssDNA in a solution, *Curr. Appl. Phys.,* 2009, 9, 534–537.

34. Y. Zhang, Z. Tang, J. Wang, H. Wu, A. Maham and Y. Lin, Label-free DNA biosensor based on SERS molecular sentinel on nanowave chip, *Anal. Chem.,* 2010, 82, 6440–6446.

35. K. C. Grabar, R. G. Freeman, M. B. Hommer and M. J. Natan, Preparation and characterization of Au colloid monolayers, *Anal. Chem.,* 1995, 67, 735-743.

36. J. Turkevich, P. C. Stevenson and J. Hillier, A study of the nucleation and growth processes in the synthesis of colloidal gold, *Discuss Faraday Soc.,* 1951, 11, 55-75.

37. P. Zhao, N. Li and D. Astruc, State of the art in gold nanoparticle synthesis, *Coord. Chem. Rev.,* 2013, 257, 638-665.

38. F. A. Tanious, B. Nguyen and W. D. Wilson, Biosensor-surface plasmon resonance methods for quantitative analysis of biomolecular interactions, *Methods Cell Biol.,* 2008, 84, 53-77.

39. S. Link and M. A. El-Sayed, Size and temperature dependence of the Plasmon absorption of colloidal gold nanoparticles, *J. Phys. Chem. B,* 1999, 103(21), 4212-4217.

40. X. Huang and M. A. El-Sayed, Gold nanoparticles: optical properties and implementations in cancer diagnosis and photothermal therapy, *Journal of Advanced Research,* 2010, 1, 13-28.

41. D. Philip, Synthesis and spectroscopic characterization of gold nanoparticles, *Spectrochim. Acta A Mol. Biomol. Spectrosc.,* 2008, 71, 80-85.

42. S. K. Sivaraman, S. Kumar and V. Santhanam, Monodisperse sub-10 nm gold nanoparticles by reversing the order of addition in Turkevich method-the role of chloroauric acid, *J. Colloid Interface Sci.,* 2011, 361, 543-547.

43. H. Liu, N. Pierre-Pierre and Q. Huo, Dynamic light scattering for gold nanorod size characterization and study of nanorod–protein interactions, *Gold Bull.,* 2012, 45, 187-195.

44. D. J. Lewis, T. M. Day, J. V. MacPherson, and Z. Pikramenou, Luminescent nanobeads: attachment of surface reactive Eu(III) complexes to gold nanoparticles, *Chem. Commun.,* 2006, 1433-1435.

45. T. A. Taton, Preparation of gold nanoparticle–DNA conjugates. DNA Nanotechnology: current protocols in nucleic acid chemistry, John Wiley and Sons, Inc, 2002, pp. 12.2.1- 12.2.12. (doi:10.1002/0471142700.nc1202s09).

46. P. Hazarika, T. Giorgi, M. Reibner, B. Ceyhan and C. M. Niemeyer, Synthesis and characterization of deoxyribonucleic acid-conjugated gold nanoparticles. Methods in molecular biology- bioconjugation protocols: strategies and methods, CM Niemeyer (ed.,) Humana Press Inc Totowa, NJ, 2004, 295-304.

47. R. Wilson, The use of gold nanoparticles in diagnostics and detection, *Chem. Soc. Rev.,* 2008, 37, 2028-2045.

48. J. C. Love, L. A. Estroff, J. K. Kriebel, R. G. Nuzzo and G. M. Whitesides, Self-assembled monolayers of thiolates on metals as a form of nanotechnology, *Chem. Rev.,* 2005, 105, 1103-1169.

49. R. A. Sperling and W. J. Parak, Surface modification, functionalization and bioconjugation of colloidal inorganic nanoparticles, *Phil. Trans. R. Soc. A,* 2010, 368, 1333-1383.

50. C. A. Widrig, C. Chung and N. D. Porter, The electrochemical desorption of n-alkanethiol monolayers from polycrystalline Au and Ag electrodes, *J. Electroanal. Chem.,* 1991, 310, 335-359.

51. S. Y. Lin, Y. Tsai, C. C. Chen, C. M. Lin and C. H. Chen, Two-step functionalization of neutral and positively charged thiols onto citrate-stabilized Au nanoparticles, *J. Phys. Chem. B,* 2004, 108, 2134-2139.

52. H. X. Li and L. J. Rothberg, Colorimetric detection of DNA sequences based on electrostatic interactions with unmodified gold nanoparticles, *Proc. Natl. Acad. Sci.,* 2004, 101, 14036-14039.

53. M. -P. N. Bui, T. J. Baek and G. H. Seong, Gold nanoparticle aggregation-based highly sensitive DNA detection using atomic force microscopy, *Anal. Bioanal. Chem.,* 2007, 388, 1185-1190.

54. K. G. Witten, J. C. Bretschneider, T. Eckert, W. Richtering and U. Simon, Assembly of DNA-functionalized gold nanoparticles studied by UV-visible spectroscopy and dynamic light scattering, *Phys. Chem. Chem. Phys.,* 2008, 10, 1870-1875.

55. C. Thiruppathiraja, S. Kamatchiammal, P. Adaikkappan, D. J. Santhosh and M. Alagar, Specific detection of *Mycobacterium sp.* genomic DNA using dual labeled gold nanoparticle based electrochemical biosensor, *Anal. Biochem.,* 2011, 417, 73-79.

56. Q. Dai, X. Liu, J. Coutts, L. Austin and Q. Huo, A one-step highly sensitive method for DNA detection using dynamic light scattering, *J. Am. Chem. Soc.,* 2008, 130, 8138-8139.

57. Y. X. Zhang, J. Zheng, G. Gao, Y. F. Kong, X. Zhi, K. Wang, X. Q. Zhang and D. X. Cui, Biosynthesis of gold nanoparticles using Chloroplasts, *Int. J. Nanomedicine,* 2011, 6, 2899-2906.

58. T. Yajima, Y. Yu and M. Futamata, Closely adjacent gold nanoparticles linked by chemisorption of neutral rhodamine 123 molecules providing enormous SERS intensity, *Phys. Chem. Chem. Phys.,* 2011, 13, 12454-12462.

59. T. Yajima, Y. Yu and M. Futamata, Steric hindrance in cationic and neutral rhodamine 6G molecules adsorbed on Au nanoparticles, *J. Raman Spectrosc.,* 2013, 44, 406-411.

60. S. Kalmodia, J. Harjwani, R. Rajeswari, W. Yang, C. J. Barrow, S. Ramaprabhu, S. Krishnakumar and S. Velchuri, Synthesis and characterization of surface enhanced Raman scattered gold nanoparticles, *Int. J. Nanomedicine,* 2013, 8, 4327-4338.

61. D. K. Lim, K. S. Jeon, J. H. Hwang, H. Kim, S. Kwon, Y. D. Suh and J. M. Nam, Highly uniform and reproducible surface-enhanced Raman scattering from DNA tailorable nanoparticles with 1-nm interior gap, *Nat. Nanotechnol.,* 2011, 6, 452-460.

62. M. M. Harper, K. S. McKeatingw and K. Faulds, Recent developments and future directions in SERS for bioanalysis, *Phys. Chem. Chem. Phys.,* 2013, 15, 5312-5328.

63. C. S. Weisbecker, M. V. Merritt and G. M. Whitesides, Molecular self-assembly of aliphatic thiols on gold colloids, *Langmuir,* 1996, 12, 3763-3772.

64. L. M. Demers, C. A. Mirkin, R. C. Mucic, R. A. Reynolds, R. L. Letsinger, R. Elghanian and G. Viswanadham, A fluorescence based method for determining the surface coverage and hybridization efficiency of thiol-capped oligonucleotides bound to gold thin films and nanoparticles, *Anal. Chem.,* 2000, 72, 5535-5541.

65. E. Y. Kim, J. Stanton, R. A. Vega, K. J. Kunstman, C. A. Mirkin and S. M. Wolinsky, A real-time PCR-based method for determining the surface coverage of thiol-capped oligonucleotides bound onto gold nanoparticles, *Nucleic Acids Res.,* 2006, 34(7), 1-7.

66. H. D. Hill, J. E. Millstone, M. J. Banholzer and C. A. Mirkin, The role of radius curvature plays in thiolated oligonucleotide loading on gold nanoparticles, *ACS Nano,* 2009, 3(2), 418-424.

67. J. J. Storhoff, R. Elghanian, R. C. Mucic, C. A. Mirkin and R. L. Letsinger, One-pot colorimetric differentiation of polynucleotides with single base imperfections using gold nanoparticle probes, *J. Am. Chem. Soc.,* 1998, 120, 1959-1964.

68. T. –T. Tsai, S. –W. Shen, C. –M. Cheng and C. –F. Chen, Paper-based tuberculosis diagnostic devices with colorimetric gold nanoparticles, *Sci. Technol. Adv. Mater.,* 2013, 14, 1-7.

69. J. J. Storhoff, A. A. Lazarides, R. C. Mucic, C. A. Mirkin, R. L. Letsinger and G. C. Schatz, What Controls the Optical Properties of DNA-Linked Gold Nanoparticle Assemblies?, *J. Am. Chem. Soc.,* 2000, 122, 4640-4650.

70. S. L. Dellaporta, J. Wood and J. B. Hicks, Experimental protocols; a plant mini preparation: Version II, *Plant Mol. Biol. Rep.,* 1983, 1, 19-21.

List of figure captions:

Figure 1. Schematic representation of colorimetric detection of ToLCNDV DNA using AuNP conjugated bi-functional oligonucleotide probe and self-assembly of gold cluster.

Figure 2. Synthesis and characterizations of citrate capped AuNPs. (A) Deep red color of synthesized citrate capped AuNPs, (B) UV-Visible spectra of citrate capped AuNPs with absorbance maximum at 520 nm, (C) HR-TEM image of spherical shaped AuNPs with ~ 19 nm in size and (D) hydrodynamic diameter of citrate capped AuNPs (~ 30 nm).

Figure 3. Preparation and characterization of AuNP conjugated bi-functional oligonucleotide probe. (A) Photographic image of AuNP-bifunctional oligonucleotide probe "a" AuNPs without NaCl treatment, "b" AuNP-bifunctional oligonucleotide probe after salt treatment and "c" Salt induced aggregated AuNPs. Corresponding UV- visible spectra (a-c) for AuNPs, AuNP-bifunctional oligonucleotide probe and aggregated AuNPs (B). (C) Surface enhanced Raman spectra of R6G, R6G with AuNP-bifunctional oligonucleotide probe and R6G with AuNPs and corresponding Raman images with scale bar. (D) HRTEM image of AuNP conjugated bi-functional oligonucleotide probe and (E) Average hydrodynamic diameter of AuNP-bifunctional oligonucleotide probe (~ 65nm).

Figure 4 Optimization of salt concentration for the complete aggregation of AuNP-bifunctional oligonucleotide probe. (A) Photographic image of aggregation of AuNP-bifunctional oligonucleotide probe at different concentrations (1- 6 M) with control "C". (B) UV-visible spectra of AuNP-bifunctional oligonucleotide probe with different concentrations of salt (C, 1-6M).

Figure 5. Hybridization of AuNP-bifunctional oligonucleotide probe with dsDNA target at different ratios (0.0- 1.0). (A) Photographic image of hybridized AuNP-bifunctional

oligonucleotide probe with dsDNA targets, (B) corresponding UV-visible absorbance spectra before the salt treatment and (C) Bargraph of degree of absorbance at 525 nm.

Figure 6. Colorimetric detection of ToLCNDV DNA using AuNP- bifunctional oligonucleotide probe. (A) Photographic image of hybridized AuNP-bifunctional oligonucleotide probe with dsDNA targets at different ratios (0.0- 1.0) after the salt treatment, (B) corresponding UV-visible absorbance spectra and (C) Bargraph of degree of absorbance at 525 nm.

Figure 7. HR-TEM images of hybridized AuNP-bifunctional oligonucleotide probe with its dsDNA target (A) and with out dsDNA target (B) after the salt treatment. dsDNA templated self assembled large AuNP cluster and aggregated AuNP-bifunctional oligonucleotide probe in the presence and absence of dsDNA target after the salt treatment, respectively.

Figure 8. DNA templated self-assembly of AuNP cluster through hybridization of AuNP-bifunctional oligonucleotide probe and dsDNA target flower and pyramid structures. An individual cluster comprising 2-11 nanoparticles as petals. Flower like cluster assembly of AuNP-bifunctional oligonucleotide probe consisting single AuNP-bifunctional oligonucleotide probe conjugate core anchored with mono (a), dimer (b), trimmers (c&d), tetramer (e), hexamer (f), octamer (g) and decamer (h). (i) Pyramid like structure assembly of AuNPs.

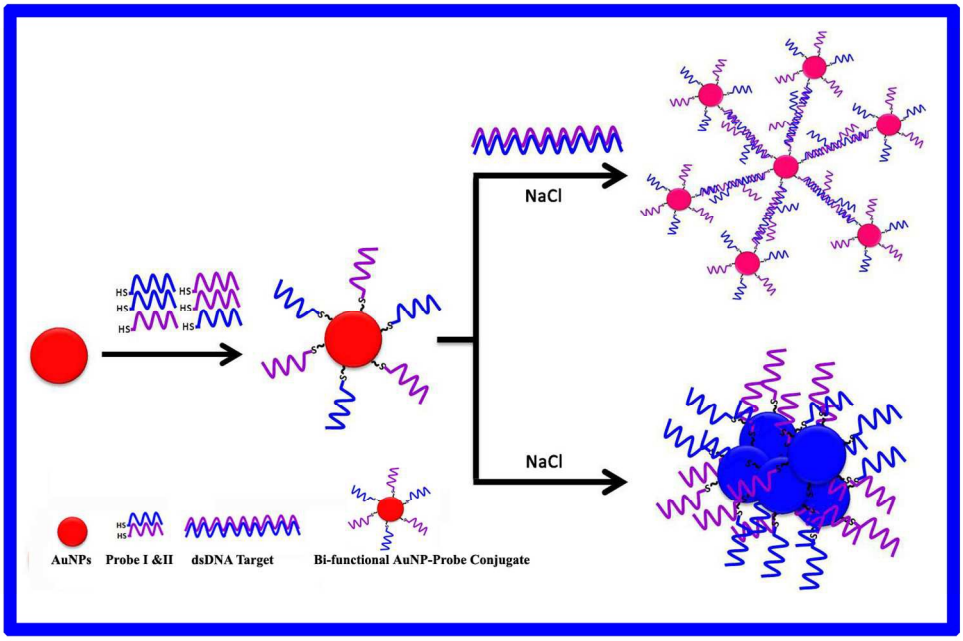

261x197mm (150 x 150 DPI)

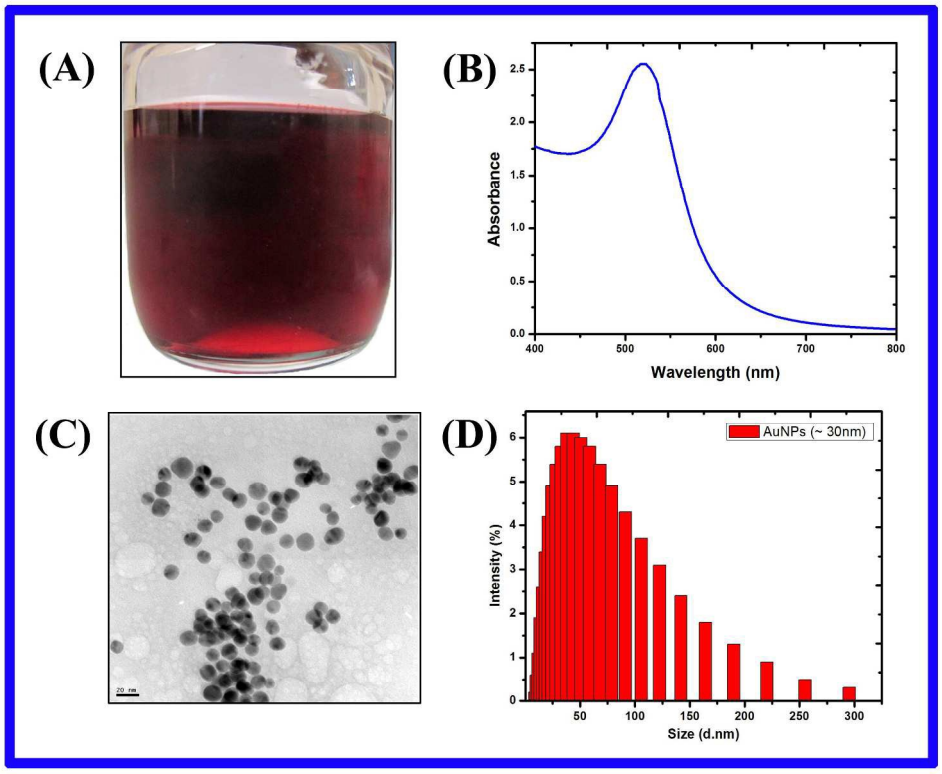

514x406mm (150 x 150 DPI)

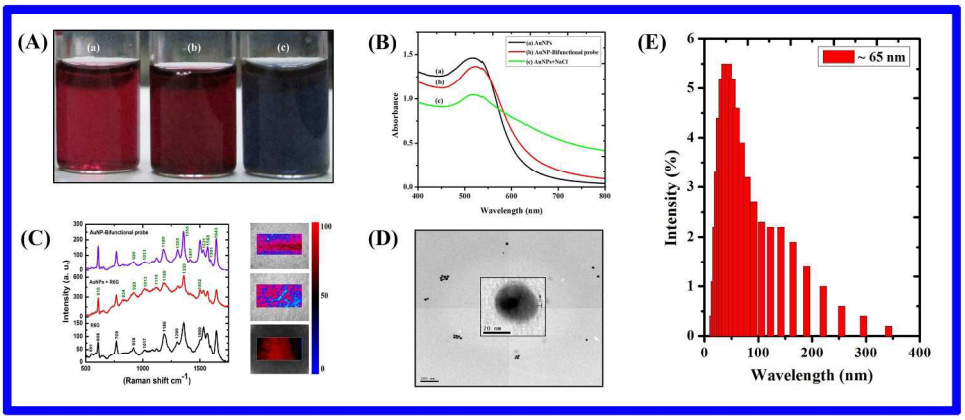

482x220mm (150 x 150 DPI)

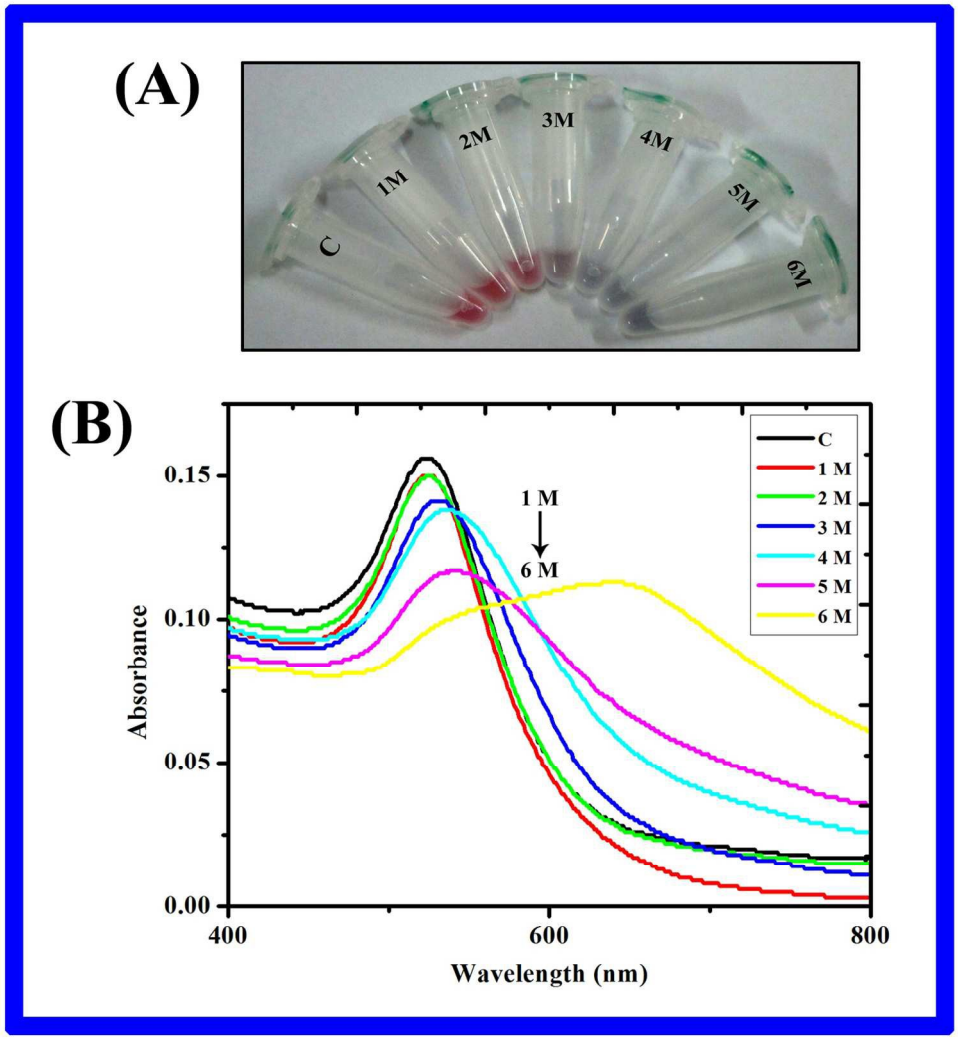

280x304mm (150 x 150 DPI)

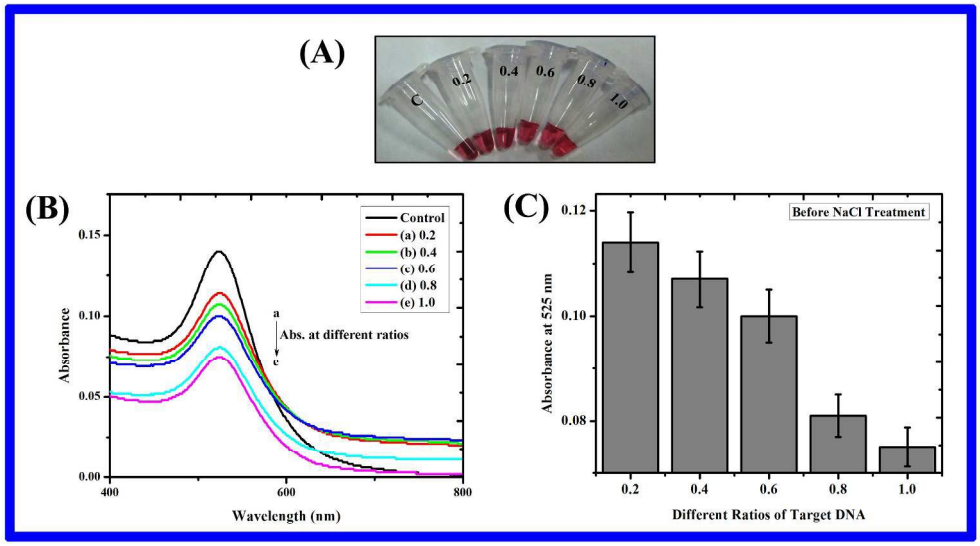

525x289mm (150 x 150 DPI)

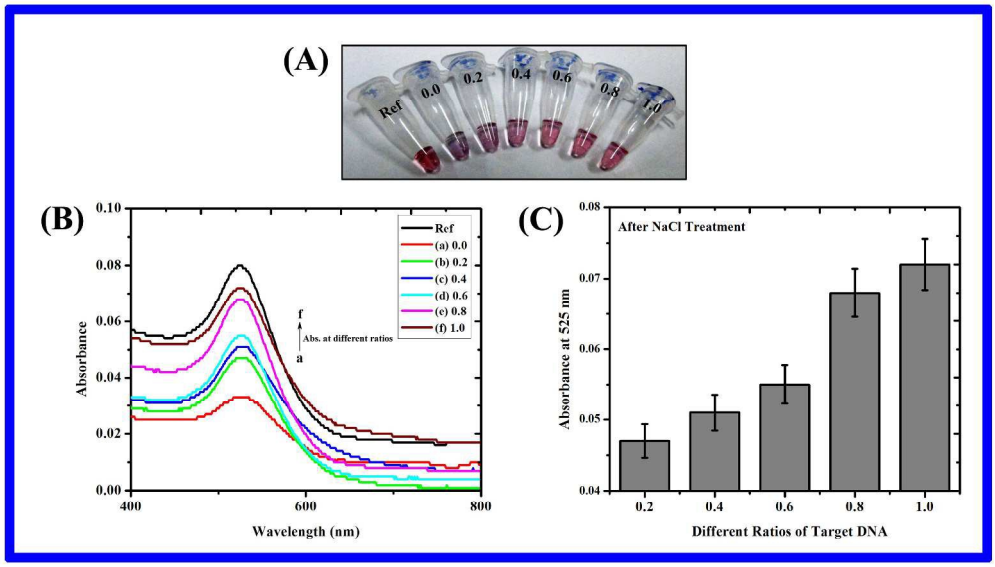

530x319mm (150 x 150 DPI)

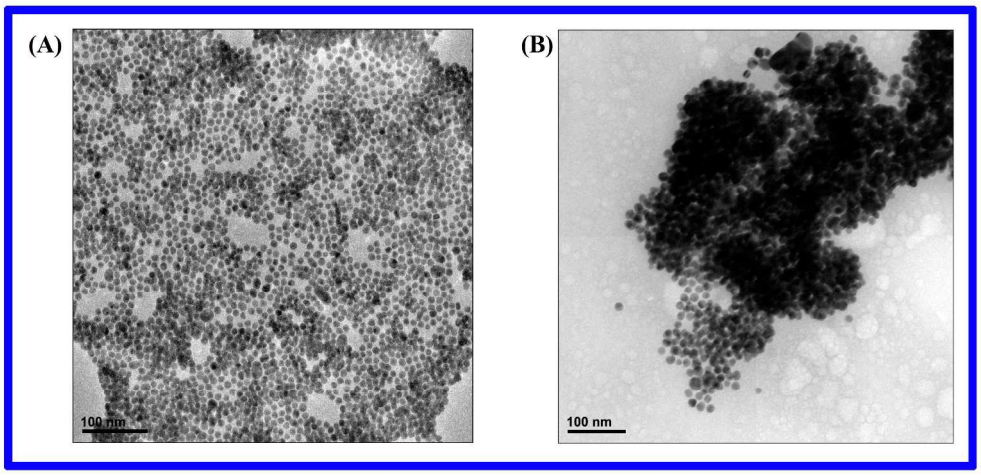

1288x635mm (72 x 72 DPI)

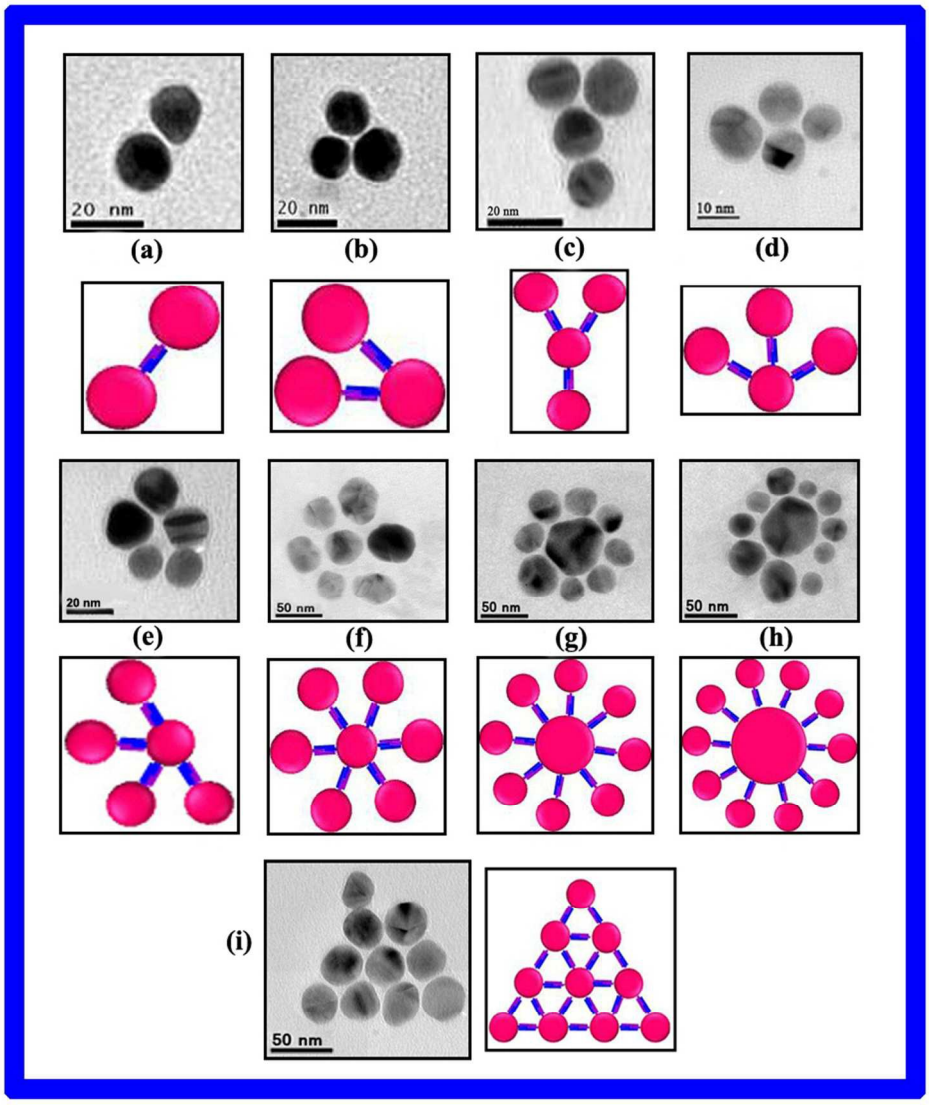

355x404mm (72 x 72 DPI)

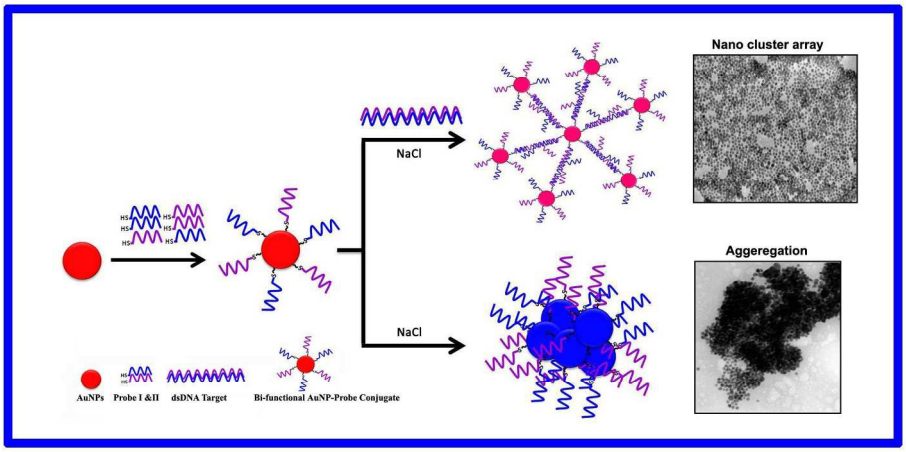

388x197mm (150 x 150 DPI)